J Mol Model (2013) 19:2459–2472
DOI 10.1007/s00894-013-1784-1

ORIGINAL PAPER

Energetics of liposomes encapsulating silica nanoparticles

Duangkamon Baowan · Henrike Peuschel · Annette Kraegeloh · Volkhard Helms

Received: 22 November 2012 / Accepted: 28 January 2013 / Published online: 24 February 2013

Abstract Nanoparticles may be taken up into cells via endocytotic processes whereby the foreign particles are encapsulated in vesicles formed by lipid bilayers. After uptake into these endocytic vesicles, intracellular targeting processes and vesicle fusion might cause transfer of the vesicle cargo into other vesicle types, e.g., early or late endosomes, lysosomes, or others. In addition, nanoparticles might be taken up as single particles or larger agglomerates and the agglomeration state of the particles might change during vesicle processing. In this study, liposomes are regarded as simple models for intracellular vesicles. We compared the energetic balance between two liposomes encapsulating each a single silica nanoparticle and a large liposome containing two silica nanoparticles. Analytical expressions were derived that show how the energy of the system depends on the particle size and the distance between the particles. We found that the electrostatic contributions to the total energy of the system are negligibly small. In contrast, the van der Waals term strongly favors arrangements where the liposome snugly fits around the nanoparticle(s). Thus the two separated small liposomes have a more favorable energy than a larger liposome encapsulating two nanoparticles.

Keywords Coulombic function · Lennard-Jones function · Liposomes · Silica nanoparticle

D. Baowan (✉)
Department of Mathematics, Faculty of Science,
Mahidol University, Rama VI Rd,
Bangkok, Thailand
e-mail: duangkamon.bao@mahidol.ac.th

D. Baowan
Centre of Excellence in Mathematics, CHE, Si Ayutthaya Rd,
Bangkok 10400, Thailand

H. Peuschel · A. Kraegeloh
Nano Cell Interactions Group, INM-Leibniz Institute
for New Materials, Campus D2 2,
66123 Saarbruecken, Germany

V. Helms
Center for Bioinformatics, Campus E2 1,
Saarland University, 66123 Saarbruecken, Germany

Introduction

The uptake of nanoparticles into living cells depends on the physicochemical properties of the particles such as size, electrostatic charge, and their hydrophobic/hydrophilic properties [1, 2]. Besides the material properties, also the cell type, the endocytosis mechanism [3–5], as well as components of the surrounding medium, such as proteins influence the uptake of nanoparticles into cells [6–8]. Upon binding to the plasma membrane, the nanoparticle may induce the formation of a vesicle so that endocytosis takes place. Once the particles are inside the cell, either in the cytoplasm or the nucleus, agglomeration of nanoparticles may occur [9–11].

Silica (SiO_2) is an inorganic material that is central for many applications in nanotechnology. In the biomedical field it may serve as a delivery system for drugs and genes [12, 13]. For example, it has been shown that surface-functionalized silica nanoparticles can deliver DNA [14–19] and drugs [13, 20–22] into animal cells and tissues. Schübbe and co-workers [11] investigated the location of SiO_2 nanoparticles of 32 nm and 83 nm in diameter within Caco-2 cells as a model of human intestinal cells and found that both types can enter into the cytoplasm. With increasing incubation time, the particles move toward the nucleus of the cells. The data indicated that close to the nucleus, besides single particles, also larger agglomerates of multiple particles are present. Using A549 cells as model for human type II alveolar epithelial cells, Schumann et al. [23], recorded the movement of silica nanoparticles present within endocytotic vesicles derived from the plasmic membrane

and other vesicles like lysosomes and large lamellar bodies, a special vesicle type, responsible for the transport of pulmonary surfactant to the cellular surface [24]. Some of these vesicles encapsulated at least two particle agglomerates [23]. The experimental data indicates binding of the particles to the inner vesicle membrane, which has also been found by others [25]. Malvindi et al. [26] found that cellular uptake of silica particles with sizes of 25, 60 and 115 nm that carried either negative or positive charges was independent of the surface charge.

A liposome is primarily composed of a lipid bilayer and it is used in this study as a model for membrane derived vesicles. It is well-known that the bending energy of the lipid shell does not depend on the liposome radius [27]. Over decades, the encapsulation of drugs or genes in liposomes has been studied for efficient and safe delivery systems. Foldvari et al. [28] proposed a hypothetical model for liposome-skin interaction and found in clinical testing that the drugs encapsulated in liposome provide sustained release. Puyal et al. [29] found that cationic liposomes have a relatively low cellular toxicity and are suitable as gene carrier. Moreover, Mohanraj et al. [30] studied a hybrid silica-liposome nanocapsule containing insulin and showed that the release rate of insulin from silica coated liposomes was reduced in comparison to uncoated liposomes. Thus a specifically engineered nanoparticle layer may allow the controlled release.

During the past two decades, various atomistic molecular mechanics force fields have been parameterized enabling the dynamic simulation of lipid bilayers [31–33]. Recently, several coarse grained models were introduced for lipid membranes [34–38] to cope with the large dimensions of membrane compartments such as liposomes. For example, Marrink et al. [35] described the parametrization of a coarse grained model for the dipalmitoylphosphatidylcholine (DPPC) lipid system. Furthermore, Shelley et al. [36] used a coarse grained model to study the structure and self-assembly of phospholipids bilayers. Another coarse-grained force field for zwitterionic lipids based on fitted thermodynamic and structural properties was developed by Shinoda et al. [38]. In the present paper, we apply the MARTINI force field for lipids proposed by Marrink et al. [35].

Besides force field descriptions for the energy of molecular conformations that use either atomistic or coarse grained descriptions, such systems can also be studied using the continuum approach. Here one assumes that discrete atomic arrangements can be replaced by a uniform atomic distribution, so that the total interaction energy between two molecules can be evaluated using an integral technique. The continuum approach has been successfully applied by a number of authors for determining the molecular interaction energy of nanostructures, see for example Girifalco et al. [39], Hodak and Girifalco [40], Cox et al. [41, 42], and Baowan et al. [43]. In the first two studies [39, 40], analytical expressions were derived for the potential energies for various arrangements of a carbon nanotube and a C_{60} fullerene. Cox et al. [41, 42] used elementary mechanical principles together with the continuum approach to study the oscillatory behavior of a C_{60} fullerene inside carbon nanotubes of various sizes. The structural behavior and oscillatory frequency obtained from their study are in good agreement with molecular dynamics simulations of Qian et al. [44] and Liu et al. [45]. Further, this approach has been adopted by one of the present authors [43] to study the penetration of a C_{60} fullerene through a lipid bilayer, where a relation between particle size, hole size and the location of the particle in the bilayer was determined.

In this paper, we aim to determine the equilibrium configurations between two simple arrangements, (i) two liposomes containing each a single silica nanoparticle and (ii) a larger liposome encapsulating two silica nanoparticles. Moreover, the energetic stabilities of the two systems around the minima are examined. By comparing the relative energy difference between these two systems, we assume that the energy contributions arising from the environment, such as the proteins and ions in the media, largely cancel out, so that they are not considered here. We apply the Coulombic potential including the Born equation to account for the solvation energy and the Lennard-Jones potential together with the continuum approximation to determine the total energies for the two systems of silica nanoparticles encapsulated in liposome(s). The surface and the volume integrals are utilized to analytically express the model calculations. Both liposome and silica nanoparticle are modeled as perfect spheres. In the following section, we introduce the energy terms including the electrostatic and the van der Waals energies, and the continuum approach that is used to determine the total energy of the system. The mathematical derivations for the interaction energy are given in section Results. Furthermore, numerical results for the two systems are presented in section Numerical results followed by a short discussion. Finally, mathematical details for the total energy and the use of the constants are given in Appendix.

Methods

This study aims at computing the energy of systems involving inorganic nanoparticles of several tens of nanometers in size and an organic lipid bilayer large enough to enclose them. This is a challenging topic since it involves a biomolecular lipid system as well as inorganic particles. Only a few authors have previously derived parameterizations for such hybrid systems [15, 22, 46]. The mere size of these systems renders an atomistic modeling approach very

expensive. Even a coarse grained particle approach would involve computing around three hundred thousands of pairwise interactions. Instead, we apply a much more efficient continuum approach that considers the same typical non-bonded interactions. Since we consider relative energy differences between two different molecular arrangements, we may assume that many interactions will cancel out. For example, we consider the case that the outer surface area of the large liposome is twice as large as that of the small liposomes. Hence, we do not consider the interactions of the lipid bilayer with the surrounding solvent because these can be considered as being proportional to the liposome surface, so that they will largely cancel out when taking the difference between both systems.

The MARTINI force field [35] is used to determine the molecular interaction energy between a liposome and an embedded silica nanoparticle. Both electrostatic and van der Waals energies are taken into account utilizing Coulombic and Lennard-Jones potential functions. The electrostatic energy for molecules carrying partial charges and the electrostatic part of their solvation free energy can be modeled using the sum of Coulombic function and Born Eq. [47]. These are given by

$$U = \frac{q_i q_j}{4\pi\epsilon_0\epsilon_r}\frac{1}{\rho} - \frac{1}{8\pi}\left(\frac{1}{\epsilon_i} - \frac{1}{\epsilon_r}\right)\frac{q_i q_j}{f_{GB}},$$

where ρ denotes the distance between two typical charge centers, q_i and q_j are partial point charges, ϵ_0 denotes the vacuum permittivity of the value $8.85\times10^{-12}\mathrm{CV}^{-1}m^{-1}$, and ϵ_i and ϵ_r are relative dielectric constants. The generalized Born equation (f_{BG}) is given by $f_{GB} = \sqrt{\rho^2 + a^2 e^{-\rho^2/(4a^2)}}$, where a is the van der Waals radius of a charged particle, and for $\rho \gg a$ we may approximate $f_{GB} = \rho$. Then, the electrostatic term becomes

$$U = \frac{q_i q_j}{4\pi}\left[\frac{1}{\epsilon_r\epsilon_0} - \frac{1}{2}\left(1 - \frac{1}{\epsilon_r}\right)\right]\frac{1}{\rho},$$

where we take ε_i=1.

The standard 6–12 Lennard-Jones function is used to describe the van der Waals energy of the system, and it is given by

$$\Phi = -\frac{A}{\rho^6} + \frac{B}{\rho^{12}} = 4\epsilon\left[-\left(\frac{\sigma}{\rho}\right)^6 + \left(\frac{\sigma}{\rho}\right)^{12}\right],$$

where A and B are attractive and repulsive Lennard-Jones constants, respectively, σ is the van der Waals diameter and ϵ denotes the van der Waals well depth. The Lennard-Jones constants between two atomic or coarse grained species can be obtained using the empirical combining laws or mixing rules [48] as $\epsilon_{12} = \sqrt{\epsilon_1\epsilon_2}$ and $\sigma_{12} = (\sigma_1 + \sigma_2)/2$, where 1 and 2 refer to the respective individual species.

Using the continuum approach [41–43], where the atoms (or coarse-grained particles) at discrete locations of the molecule are averaged over a surface or a volume, the molecular interatomic energy is obtained by calculating integrals over the surface or the volume of each molecule, given by

$$E = \eta_1\eta_2\int_{S_1}\int_{S_2}\left\{\frac{q_i q_j}{4\pi}\left[\frac{1}{\epsilon_r\epsilon_0} - \frac{1}{2}\left(1 - \frac{1}{\epsilon_r}\right)\right]\frac{1}{\rho} + \left(-\frac{A}{\rho^6} + \frac{B}{\rho^{12}}\right)\right\}dS_2 dS_1,$$

where η_1 and η_2 represent the average surface density or the average volume density of atoms on each molecule. For the surface and volume integrals computed in this work it is convenient to define the integral I_n as

$$I_n = \int_{S_1}\int_{S_2}\rho^{-2n}dS_2 dS_1, \quad n = 1/2, 3, 6. \tag{1}$$

Written in this way, the integral corresponds to scaled versions of the above energy terms.

The Coulombic and Lennard-Jones constants for silica are taken from the work of Cruz-Chu et al. [49] whereas those for the lipid bilayer are taken from the work of Marrink et al. [35]. Amorphous silica nanoparticles are composed of SiO_2, with the silicon atoms in tetrahedral coordination with four oxygen atoms and a random connection of the tetrahedra. Upon contact with water, silanol groups (SiOH) are formed on the particle surface [50, 51]. Following the notation of the MARTINI model, a silica nanoparticle is assumed to be a spherical molecule with a medium-strength polarity of 3 (P_3) where the parameters for P_3 are given in Table 1 of Marrink et al. [35]. Further, its inside is assumed to comprised of small SiO_2 beads carrying no charges whereas the outer surface of the solvated nanoparticle is partially covered by silanol (−SiOH) groups [49, 52]. Following the work of Cruz-Chu et al. [49], the densities of the dangling atoms of silicon and oxygen are approximately 1 nm^{-2}. Therefore, to guarantee the neutral charge of the silica nanoparticle, we treat the hydroxyl group as a united atom and make it slightly less polar than the -OH group of a water molecule in typical atomic force fields. Thus, the partial charges for the silicon atom and the hydroxyl group of silanol groups are taken as +0.3|e| and –0.3|e|, respectively.

A liposome is assumed to be composed of dipalmitoylphosphatidylcholine (DPPC) lipids that are represented in the MARTINI force field by a head group, consisting of choline (Q_0) and phosphate (Q_a) groups, a glycerol group (N_a) and a tail group (C_1) [35]. In this paper, the spacing between the two layers of lipids is assumed to be 0.334 nm [43]. The positions for choline, phosphate and glycerol groups are taken as ±2.165 nm, ±2.118 nm and ± 1.768 nm, respectively, from the center of the bilayer following the work of Petrache et al. [53], compare the insert diagram of Fig. 2. The Coulombic and Lennard-Jones

Table 1 Coulombic and Lennard-Jones parameters for silica nanoparticle and liposome used in this model

Atom type	q (C)	ε (kJ mol^{-1})	σ (nm)	Dangling atom density (nm^{-2})
Si	0 $\|e\|$	1.297	0.4295	–
O	0 $\|e\|$	0.628	0.3500	–
$Si_{silanol}$	+0.30 $\|e\|$	1.297	0.4295	1.00
$O_{silanol}$	−0.30 $\|e\|$	0.628	0.3500	1.00
Q_a	−1.00 $\|e\|$	5.600	0.4700	–
Q_o	+1.00 $\|e\|$	5.000	0.4700	–
N_a	–	4.500	0.4700	–
C_1	–	2.300	0.4700	–

parameters for both silica nanoparticle and liposome used here are summarized in Table 1.

Further, the number of lipid molecules per liposome is determined as the sum of the lipids in the outer and inner layers, and it is given by

$$N_{lipids}(r) = \frac{4\pi r^2 + 4\pi(r-h)^2}{A},$$

where r is the outer radius of the liposome, h denotes the thickness of the bilayer, which is taken to be 4.336 nm, and A represents the lipid head group area, which is 0.64 nm^2 for DPPC lipids [35]. The coarse grained model assigns two interaction sites to the head group, one for the choline group and one for the phosphate group, two interaction sites to the intermediate layer of the glycerol group and eight interaction sites to the tail group [35]. We assume that the intermediate group of the liposome can be represented as a spherical surface, so that the average atomic surface density for the intermediate group, η_{si}, is given by $2N_{lipids}(r)/(4\pi r^2)$. Here, the factor 2 reflects that two interaction sites are used for the intermediate layer in the MARTINI force field. Also the tail group is approximated as a spherical shell with a thickness of a tail length ℓ, and the average atomic volume density for the tail group, η_{vt}, is given by $8N_{lipids}(r)/[(4\pi r^3)/3]$. Again, the factor 8 reflects the eight interaction sites of the tail group. Along the same line, the head group can be modeled either as a spherical surface or as a spherical shell with a thickness of 0.4 nm. Consequently, both average atomic surface and average atomic volume densities of the head group, η_{sh} and η_{vh}, can be determined in the same way as described for the intermediate and the tail groups.

Here, the average atomic surface density of silica, η_{silica}, may be obtained as $3/[4\ \pi\ (0.161)^2]$ nm^{-2}, where 3 is the number of atoms in a molecule, and assuming that the Si atom is located at the center whereby the bond length between Si and O is 0.161 nm. One third of this value is assigned to the distribution of silicon atoms, and two thirds of this value represent the atomic distribution of oxygen atoms.

We note that the silica nanoparticle is introduced here as a model particle to illustrate the physical properties such as size and charge of nanoparticles. Once the particle type is replaced by another material, only the parameters and constants need to be changed, but the mathematical expressions derived in the Results section remain the same.

Results

In this study, a surface integration technique is applied to evaluate the total energy for one or two nanoparticles encapsulated in a liposome. Both SiO_2 nanoparticle and liposome are modeled as perfect spheres where the atoms on each molecule are uniformly distributed over the surface or the volume of the sphere. First, we consider the interaction between a single atom and a sphere using the surface integral approach. Then the single atom is assumed to belong to the other molecules. Five different possible molecular configurations are shown in Fig. 1. Either the surface or the volume integral is used to determine the total energy of the system.

Coulombic function

For this we consider the integral I_n defined in Eq. (1) with $n = 1/2$. In the case of a spherical surface with radius a interacting with a single atom, as depicted in Fig. 1(a), the distance from a typical surface element on the sphere to the atom is given by $\rho^2 = (a\cos\theta\sin\phi)^2 + (a\sin\theta\sin\phi)^2 + (a\cos\phi - \delta)^2$, and we may deduce

$$\begin{aligned} I_{1/2} = \int_s \frac{1}{\rho} dS &= \int_{-\pi}^{\pi}\int_0^{\pi} \frac{a^2\sin\phi}{\left(a^2+\delta^2-2a\delta\cos\phi\right)^{1/2}} d\phi d\theta \\ &= \frac{\pi a}{\delta}\int_{(\delta-a)^2}^{(\delta+a)^2} \frac{1}{\sqrt{t}} dt \\ &= 4\pi a^2 \frac{1}{\delta}, \end{aligned} \tag{2}$$

where δ is the distance from the center of the sphere to the atom. Here, we substituted $t = a^2 + \delta^2 - 2a\delta\cos\phi$ to transform ϕ to t in the first integration. The finding that the Coulombic interaction decays with the inverse distance $1/\delta$ is a text book example for the electrostatic interaction around a charged sphere. The scaling with the square of the particle radius a reflects that, assuming a

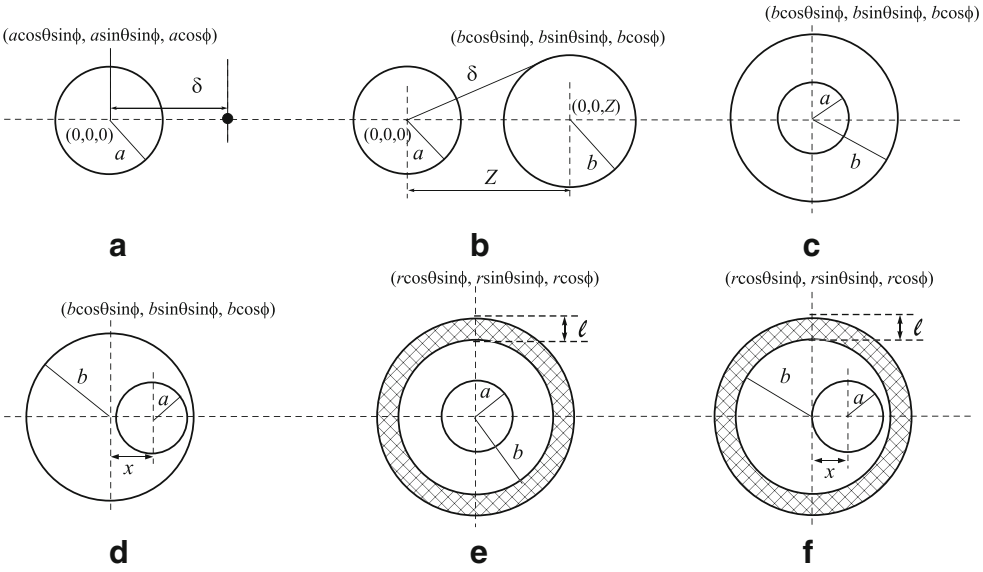

Fig. 1 Schematic structures for (**a**) a sphere interacting with a single atom, (**b**) offset spheres, (**c**) concentric spheres and (**d**) offset of concentric spheres for the outer surface integral, and (**e**) concentric spheres and (**f**) offset of concentric spheres for the outer volume integral

constant surface density of charge centers, the number of charge centers is proportional to the particle surface. Next we aim to integrate $1/\delta$ over another spherical structure for the offset and the concentric configurations.

In the case of a pair of offset spheres as shown in Fig. 1(b), the distance δ from the center of the first sphere to a typical surface element on the second sphere of radius b is given by $\delta^2 = (b\cos\theta\sin\phi)^2 + (b\sin\theta\sin\phi)^2 + (b\cos\phi - Z)^2$. Hence, the total electrostatic energy can be written as

$$U = \frac{q_i q_j}{4\pi}\left[\frac{1}{\epsilon_r\epsilon_0} - \frac{1}{2}\left(1 - \frac{1}{\epsilon_r}\right)\right] K^{Q}_{1/2}(a,b),$$

where

$$K^{Q}_{1/2}(a,b) = 4\pi a^2 \int_S \frac{1}{\delta} dS = 4\pi a^2 \int_{-\pi}^{\pi}\int_0^{\pi} \frac{b^2\sin\phi}{(b^2+Z^2-2bZ\cos\phi)^{1/2}} d\phi d\theta = 16\pi^2 a^2 b^2 \frac{1}{Z}, \tag{3}$$

and Z is the distance between their centers. This case can be easily understood as an extension of the first case.

In the case of concentric spheres as shown in Fig. 1(c), we start from (2) and take $\delta = b$, and we may deduce

$$L^{Q}_{1/2}(a,b) = 4\pi a^2 \int_S \frac{1}{\delta} dS = 4\pi a^2 \int_{-\pi}^{\pi}\int_0^{\pi} \frac{b^2\sin\phi}{b} d\phi d\theta = 16\pi^2 a^2 b. \tag{4}$$

When the inner sphere is displaced, see Fig. 1(d), the energy remains unchanged. In this case, we have $\delta^2 = b^2 + x^2 - 2bx\cos\phi$ and then we may deduce

$$M^{Q}_{1/2}(a,b) = 4\pi a^2 \int_S \frac{1}{\delta} dS = 4\pi a^2 \int_{-\pi}^{\pi}\int_0^{\pi} \frac{b^2\sin\phi}{(b^2+x^2-2bx\cos\phi)^{1/2}} d\phi d\theta = 16\pi^2 a^2 b. \tag{5}$$

We see that $L^{Q}_{1/2}(a,b)$ defined by (4) and $M^{Q}_{1/2}(a,b)$ defined by (5) are equal. Consequently further in the text we will use $L^{Q}_{1/2}(a,b)$ to refer to $M^{Q}_{1/2}(a,b)$. This is a well-known result since the electrostatic potential inside an isotropically charged sphere is constant.

The two cases shown in Fig. 1(e) and (f) with a finite thickness of the surface yield the same results for the Coulombic potential.

Lennard-jones function

We begin by considering the integral I_n defined by (1) for n=3, 6 and for a spherical molecule of radius a centered at the origin and a point located at $(0,0,\delta)$, as shown in Fig. 1(a). Following the work by Cox et al. [41], it is convenient to express the surface integral I_3 and I_6 in terms of J_n which is defined by $J_n = 1/\left(\delta^2 - a^2\right)^n$ where n is a positive integer corresponding to the power of the polynomials appearing in I_3 and I_6 defined by (6) and (7), respectively. This gives

$$I_3[J_n] = 4\pi a^2\left(J_3 + 2a^2 J_4\right), \tag{6}$$

$$I_6[J_n] = \frac{4}{5}\pi a^2\left(5J_6 + 80a^2 J_7 + 336a^4 J_8 + 512a^6 J_9 + 256a^8 J_{10}\right). \tag{7}$$

Next, we consider the offset spheres as shown in Fig. 1(b) where we need to evaluate a surface integral for J_n. Similar to the case of the Coulombic function, the distance δ is given by $\delta^2 = b^2 + Z^2 - 2bZ\cos\phi$. Thus we may deduce

$$K^{LJ}_{n}(a,b) = \int_S J_n dS = \int_{-\pi}^{\pi}\int_0^{\pi} \frac{b^2\sin\phi}{(b^2+Z^2-2bZ\cos\phi-a^2)^n} d\phi d\theta = \frac{\pi b}{Z(n-1)}\left[\frac{1}{\left[(Z-b)^2-a^2\right]^{n-1}} - \frac{1}{\left[(Z+b)^2-a^2\right]^{n-1}}\right], \tag{8}$$

where Z is the distance between the two centers of the two spheres and $Z > b$.

Figure 1(c) shows a schematic model for the surface interaction between two concentric spheres. In this case the distance $\delta = b$, and the integration is straightforward performed as

$$L_n^{LJ}(a,b) = \int_S J_n dS = \int_{-\pi}^{\pi}\int_0^{\pi} \frac{b^2\sin\phi}{(b^2-a^2)^n} d\phi d\theta = \frac{4\pi b^2}{(b^2-a^2)^n}. \quad (9)$$

Once the inner sphere moves away from the center with distance x as depicted in Fig. 1(d), the distance from the center of the inner sphere to a typical point on the surface of the outer sphere is given by $\delta^2 = b^2 + x^2 - 2bx\cos\phi$. By using the surface integral approach, we may deduce

$$M_n^{LJ}(a,b) = \int_S J_n dS = \int_{-\pi}^{\pi}\int_0^{\pi} \frac{b^2\sin\phi}{(b^2+x^2-2bx\cos\phi-a^2)^n} d\phi d\theta = \frac{\pi b}{x(n-1)}\left[\frac{1}{\left[(b-x)^2-a^2\right]^{n-1}} - \frac{1}{\left[(b+x)^2-a^2\right]^{n-1}}\right], \quad (10)$$

where x represents the distance between their centers and $x < b$. This equation has the same form as Eq. (8) when replacing x by Z.

In the case of the spherical volume integral for the outer sphere as shown in Fig. 1(e), the distance $\delta = r$ and we may deduce

$$N_n^{LJ}(a,b,\ell) = \int_S J_n dS = \int_{-\pi}^{\pi}\int_b^{b+\ell}\int_0^{\pi} \frac{r^2\sin\phi}{(r^2-a^2)^n} d\phi dr d\theta = \frac{4\pi(-1)^n}{a^{2n-3}} \int_{\sin^{-1}(b/a)}^{\sin^{-1}[(b+\ell)/a]} \left[\frac{1}{\cos^{2n-1}(t)} - \frac{1}{\cos^{2n-3}(t)}\right] dt, \quad (11)$$

where ℓ is the thickness of the outer ring, and for any given value of n, an analytic expression of $N_n^{LJ}(a,b,\ell)$ can be obtained.

Figure 1(f) illustrates the configuration when the inner sphere moves away from the origin about a distance x, so that $\delta^2 = r^2 + x^2 - 2rx\cos\phi$. We need to evaluate the volume integral for the outer sphere for $r \in (b, b+\ell)$ which can be written as

$$O_n^{LJ}(a,b,\ell) = \int_S J_n dS = \int_{-\pi}^{\pi}\int_b^{b+\ell}\int_0^{\pi} \frac{r^2\sin\phi}{(r^2+x^2-2rx\cos\phi-a^2)^n} d\phi dr d\theta = \frac{\pi}{x(n-1)} \int_b^{b+\ell} r\left[\frac{1}{\left[(r-x)^2-a^2\right]^{n-1}} - \frac{1}{\left[(r+x)^2-a^2\right]^{n-1}}\right] dr. \quad (12)$$

In the following sections, the mathematical expressions obtained in section Coulombic function and section Lennard-jones function will be combined to compare the total energy for a liposome encapsulating a silica nanoparticle and a liposome encapsulating two silica nanoparticles, respectively.

A liposome encapsulating a silica nanoparticle

In this section, we aim to find the equilibrium configuration for a liposome encapsulating a silica nanoparticle by minimizing the energy of the system. The schematic model is shown in Fig. 2. We consider cases where the nanoparticle is either concentric or displaced from the center toward the lipid membrane and the inner radius of the liposome, meaning the position of the inward pointing choline group, is denoted by b_1. The nanoparticle has a radius a which describes where the probability distribution of silicon atoms on the spherical surface decays to zero. Due to the fact that the bond length between silicon and oxygen in silica is around 0.161 nm [49], the probability distribution of oxygen atoms (or hydroxyl group) of the SiO_2 nanoparticles is assumed to extend to the spherical surface of radius a+0.161 nm. The fine-structure of the lipid bilayer is shown in the insert diagram of Fig. 2. Therefore, the interaction energy of the system consists of:

1. The electrostatic interaction between the inner and outer lipid head groups and the nanoparticle, based on $L_{1/2}^{Q}(a,b)$ given by Eq. (4).
2. The van der Waals interaction between the inner and outer lipid head groups and the nanoparticle, based on $N_n^{LJ}(a,b,\ell)$ given by (11).

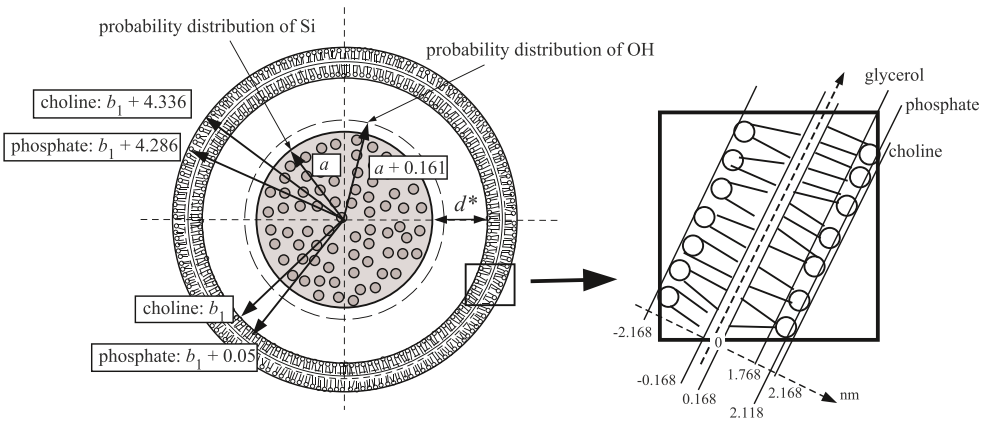

Fig. 2 Model for a silica nanoparticle encapsulated in a liposome. The right picture illustrates how the structural dimensions of the lipid bilayer are considered

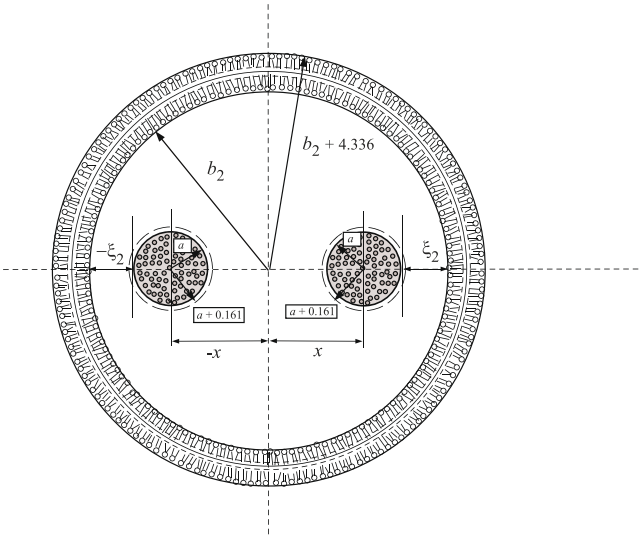

Fig. 3 Model for one liposome encapsulating two SiO_2 nanoparticles

3. The van der Waals interaction between the two intermediate lipid layers and the nanoparticle, based on $L_n^{LJ}(a,b)$ given by (9).
4. The van der Waals interaction between the inner and outer lipid tail groups and the nanoparticle, based on $N_n^{LJ}(a,b,\ell)$ defined by (11).

All the energy contributions will be scaled by appropriate coefficients according to the Coulomb, Born and Lennard-Jones equations and by the proportion of the atomic species on the molecules to yield the total energy of the system.

A liposome encapsulating two silica nanoparticles

In the rectangular Cartesian coordinate system, the liposome is assumed to be centered at the origin, and the two silica nanoparticles are centered on the x-axis at distances x and $-x$ from the origin. The physical dimensions for both liposome and silica are as described in section "A liposome encapsulating a silica nanoparticle" and the inner radius of the liposome is denoted by b_2, see Fig. 3. Therefore, the total energy for one liposome encapsulating two SiO_2 nanoparticles comprises:

1. The electrostatic interaction between the inner and outer lipid head groups and the two nanoparticles, based on $L_{1/2}^{Q}(a,b)$ given by (4).
2. The electrostatic interaction between two offset spherical SiO_2 nanoparticles, based on $K_{1/2}^{Q}(a,b)$ defined by (3) and $Z=2x$.
3. The van der Waals interaction between the inner and outer lipid head groups and the two nanoparticles, based on $O_n^{LJ}(a,\ b,\ \ell)$ defined by (12).
4. The van der Waals interaction between the two intermediate lipid layers and the two nanoparticles, based on $M_n^{LJ}(a,\ b)$ given by (10).
5. The van der Waals interaction between the inner and outer lipid tail groups and the two nanoparticles, based on $O_n^{LJ}(a,\ b,\ \ell)$ defined by (12).
6. The van der Waals interaction between two offset spherical silica nanoparticles, based on $K_n^{LJ}(a,\ b)$ defined by (8) and $Z=2x$.

We note that terms 1., 3., 4. and 5. will be multiplied by 2 to represent the fact that there are two nanoparticles encapsulated inside a liposome. Again, the total energy of the system can be obtained by scaling each energy contribution by either Coulombic and Born equation or Lennard-Jones coefficients and by the proportion of the atomic species on the molecules.

Two liposomes encapsulating a silica nanoparticle each

As for the other two cases, we derive the equilibrium position of two identical liposomes encapsulating SiO_2 nanoparticles by minimizing the energy of the system. The schematic model is shown in Fig. 4. The model description

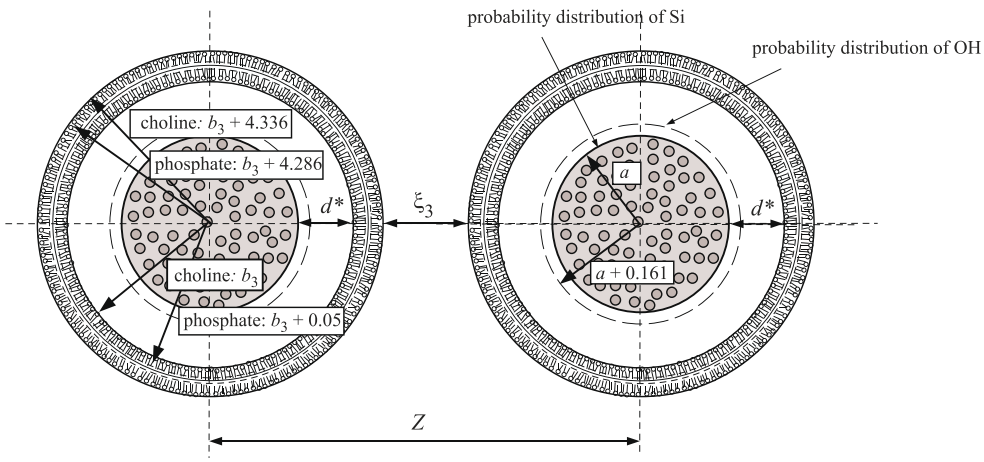

Fig. 4 Model for two silica nanoparticles encapsulated each in a liposome

for the single liposome encapsulating a silica nanoparticle is as described in section A liposome encapsulating a silica nanoparticle where b_3 denotes the inner radius of the liposome. Therefore, the interaction energy of the system consists of twice the interaction between each nanoparticle and the surrounding liposome as well as of:

1. The electrostatic interaction between two offset spherical liposomes, based on $K^{Q}_{1/2}(a,b)$ defined by (3).
2. The van der Waals interaction between two offset spherical liposomes, based on $K^{LJ}_{n}(a,b)$ defined by (8).

Note that we neglect here the interactions between the two nanoparticles because they are small compared to the interaction energy between the two liposomes.

Numerical results

Using the analytical expressions derived in Results, we now present numerical energies for three systems consisting of (i) a liposome encapsulating a silica nanoparticle, (ii) a large liposome encapsulating two silica nanoparticles and (iii) two

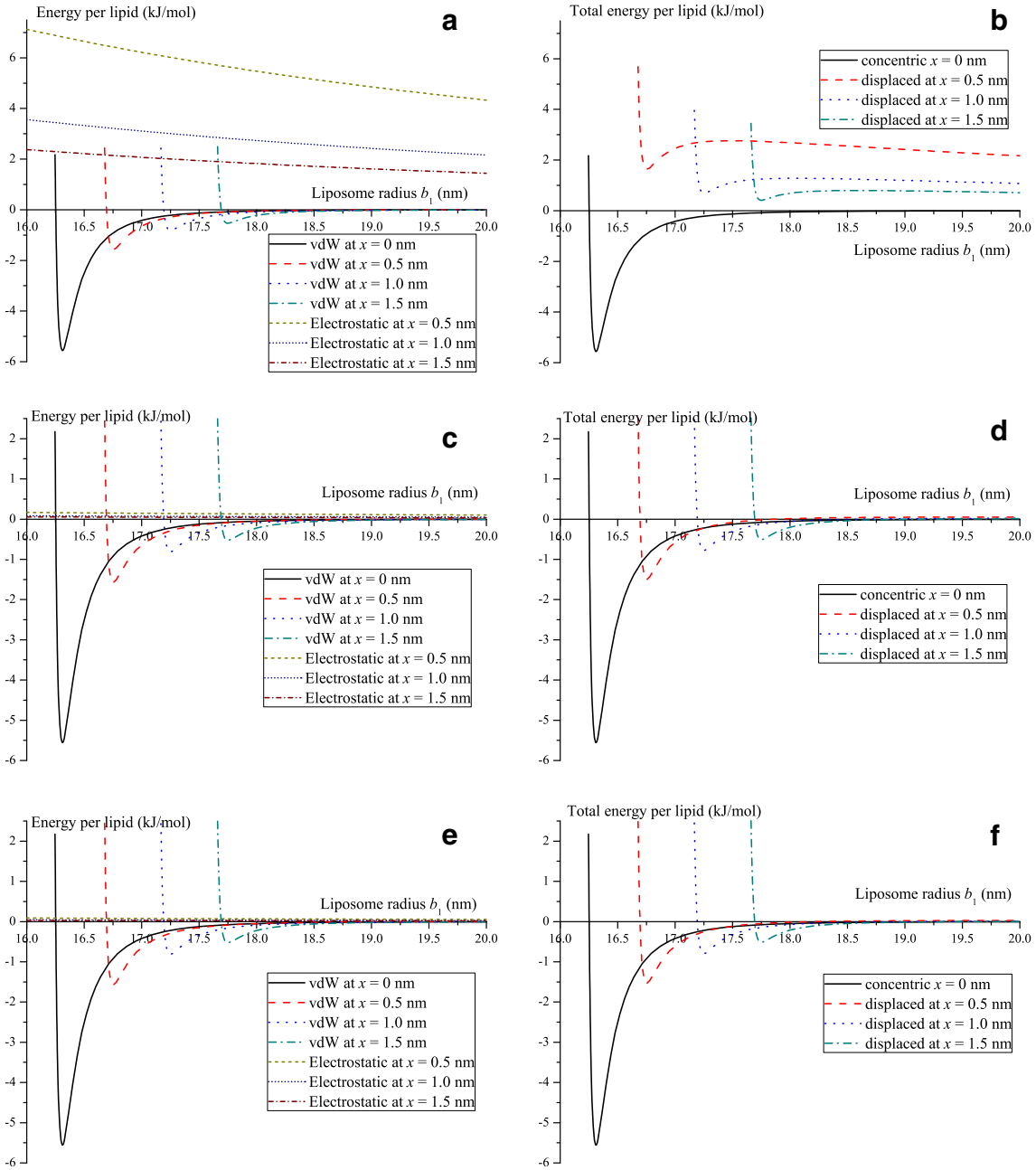

Fig. 5 Energy per lipid for a liposome encapsulating a silica nanoparticle of radius 16 nm that is placed either concentric or displaced from the liposome center by distances of 0, 0.5, 1.0 and 1.5 nm with three assumed ϵ_r values which are ϵ_r=1 (**a**), (**b**), ϵ_r=42.5 (**c**), (**d**) and ϵ_r=80 (**e**), (**f**)

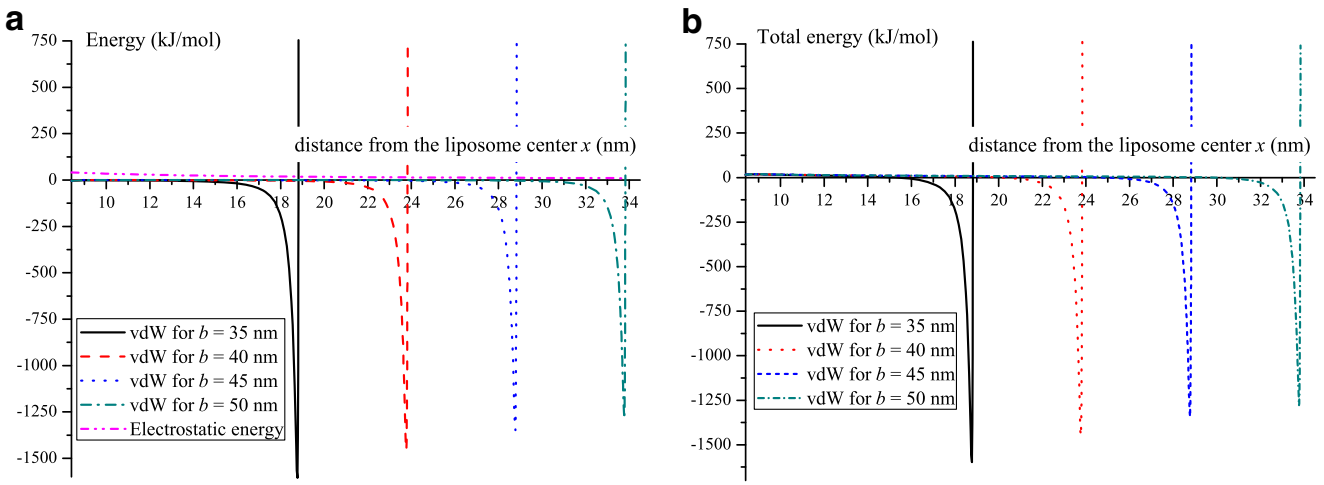

Fig. 6 (**a**) Electrostatic and van der Waals energies and (**b**) total energy profiles for a larger liposome encapsulating two silica nanoparticles with ϵ_r=80

liposomes each encapsulating a silica nanoparticle. Following the work of Schübbe et al. [11], we assume that the SiO_2 nanoparticles have a radius of a=16 nm. The charges on the zwitterionic DPPC lipids are taken as $-1|e|$ for the phosphate and $+1|e|$ for the choline groups. Further, in order to compare the systems of one large liposome and two small liposomes, the surface area of the larger liposome is set equal to the sum of the two smaller surface areas.

Figure 5 shows the energy profiles per lipid for a silica nanoparticle of 16 nm radius encapsulated inside a liposome. The particle is assumed to be either concentric or displaced from the liposome center by distances of 0, 0.5, 1.0 and 1.5 nm. Here we consider three values of the relative dielectric constant of the solvent, namely ϵ_r=1 for vacuum, see Fig. 5(a) and (b), ϵ_r=42.5 for glycerol at 25 °C, see Fig. 5(c) and (d), and ϵ=80 for water, see Fig. 5(e) and (f).

As expected, the van der Waals interactions did not depend on the value of dielectric constant but it was sensitive to the position of the nanoparticle, see Fig. 5(a), (c) and (e). On assuming that nanoparticle-solvent/membrane-solvent and solvent-solvent/nanoparticle-membrane interactions are balancing each other, we may set the van der Waals energy to zero and consider only the electrostatic energy. In vacuum, we found that the electrostatic energy of the system takes on large values and gives rise to a positive total energy of the system. This implies that the encapsulation process will not occur in the vacuum. In the other cases mimicking glycerol or water solvents, the electrostatic interaction was found to be close to zero due to the overall neutral charges of both liposome and silica nanoparticle. We note that there is a singularity of the electrostatic energy for the concentric configuration at x=0.

Furthermore, we found that the concentric configuration gives rise to the most stable arrangement among the four cases determined here, where the optimum radius of the liposome b_1 is approximately 16.31 nm around the nanoparticle of 16 nm radius. The total energy level decreases as the nanoparticle moves away from the liposome center. Moreover, we observed that the charge values of the liposome will not change the equilibrium location of the particles but will only change the magnitude of the energy level.

In order to compare the systems of one large liposome and two small liposomes, the surface area of the larger liposome is set to be equal to the sum of the two smaller surface areas. The radius of the large liposome is denoted by b_2 and that for the small liposomes is represented by b_3. Here, the energy profile for the system in water is graphically shown as a representative system where the dielectric constant $_r$ is taken to be 80 as the relative permittivity of water.

The van der Waals and the electrostatic energies for one large liposome encapsulating two silica nanoparticles are depicted in Fig. 6(a) for four assumed radii of the liposome and the fixed radius of the nanoparticle. Here, the two nanoparticles are allowed to move only in the x-direction and they are assumed to be symmetrically displaced from the liposome center. We obtained a positive energy from the electrostatic part, which reflects the repulsion energy between

Table 2 Numerical results for a larger liposome encapsulating two silica nanoparticles where x^{min} (nm) is the distance between the liposome center and the silica center in the positive x-direction at the equilibrium position

b_2	ϵ_r=1			ϵ_r=42.5			ϵ_r=80		
	E_2^{min}	x^{min}	ξ_2	E_2^{min}	x^{min}	ξ_2	E_2^{min}	x^{min}	ξ_2
35.00	−873.44	18.77	0.23	−1586.82	18.77	0.23	−1594.24	18.76	0.24
40.00	−880.26	23.77	0.23	−1443.08	23.76	0.24	−1450.23	23.76	0.24
45.00	−869.67	28.78	0.22	−1336.95	28.78	0.22	−1342.64	28.77	0.23
50.00	−875.50	33.77	0.23	−1273.00	33.77	0.23	−1279.20	33.78	0.22

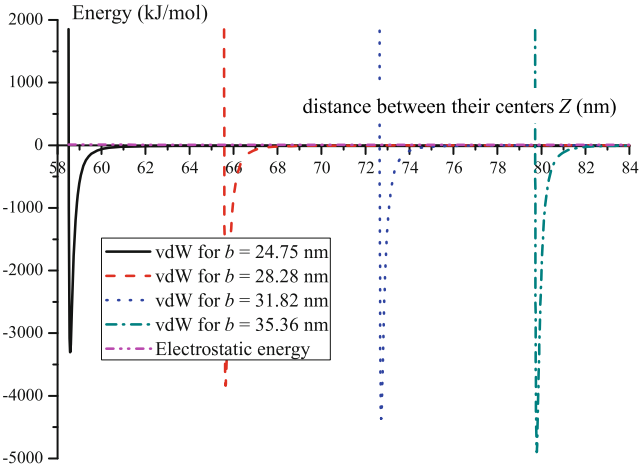

Fig. 7 Electrostatic and van der Waals energies for two liposomes encapsulating each a silica nanoparticle with ϵ_r=80. Note that the electrostatic energy is at most 8.8 kJ mol^{-1}

two identical silica nanoparticles that does of course not depend on the radius of the liposome. In terms of the van der Waals interaction, the energy at the equilibrium location is negative and it is the main energy contribution to the system.

Figure 6(b) shows the total energy of the system, and the equilibrium location is determined at the global minimum energy E_2^{min} (kJ mol^{-1}). The total energy is plotted as a function of the distance x (nm), which is defined as the distance between the liposome center and the silica nanoparticle center in the positive direction. Further, we define ξ_2 (nm) as the closest spacing between the inner surface of the liposome and the surface of the nanoparticle. The value of ξ_2 is approximately 0.23 nm for the cases studied here. The numerical results where one liposome encapsulates two silica nanoparticles for ϵ_r=1,42.5 and 80 are presented in Table 2. We found that the total energy at the equilibrium location is negative. The larger the liposome, the smaller in magnitude is the well depth.

Finally, we considered the case of two smaller liposomes containing one nanoparticle each. Figure 7 shows the energy profiles arising from the electrostatic and the van der Waals interactions. The minima of the van der Waals energy reflect configurations where the two liposomes touch. Reducing the distance between the liposome centers leads to penetrations and thus to a sharp increase of the van der Waals energy. Similar to the case of a liposome encapsulating a nanoparticle, the electrostatic energy is close to zero due to the overall neutral charges on the two molecules. At the equilibrium position, the well depth of the van der Waals energy increases as the liposome radius b_3 is increased. This reflects the increase in the amount of interacting matter.

The energy profiles and the numerical results for two liposomes encapsulating a silica nanoparticle are presented in Fig. 7 and Table 3, respectively. The b_3 values listed in Table 3 are chosen appropriately so that the small liposomes have half the surface as the larger liposomes considered in Table 2. The equilibrium position between the two liposomes is obtained where the minimum energy is denoted by E_3^{min} (kJ mol^{-1}). Moreover, the closest spacing ξ_3 (nm) between two outer surfaces of the two liposomes is in the range of 0.39–0.42 nm. The energy minima of Table 3 are at least twice as favorable as those of Table 2. Whereas the two separated liposomes have deeper and deeper energy minima for increasing radii, that of the large liposome with two nanoparticles becomes more unfavorable with increasing size.

As mentioned before, the summation of the total energy ignores a number of important contributions that are assumed to cancel out when considering the relative energy difference of the two systems. We found that the system of two separate liposomes has a more favorable energy suggesting that it may be observable in the experiment. The fix position of a single silica molecule at the center of a liposome is a best fit configuration since the spacing between the two surfaces is equal throughout the spheres. However, in the case of two silica particles inside a large spherical liposome, the spacings in y- and z-directions are larger than that in x-direction (axial direction), and therefore, at a typical point on the surface of silica, the repulsive and the attractive energies do not balance.

Our finding is in good agreement with the experimental study carried out by Chu et al. [54]. For short incubation times, they found a single silica nanoparticle in endo-lysosomes. Upon increasing the incubation duration, small organelles containing the nanoparticles will join together and form a cluster of nanoparticles in a larger endo-lysosome.

Discussion

This study presents an energetic evaluation for the encapsulation of one or two silica nanoparticles in a liposome. For

Table 3 Numerical results for two liposomes encapsulating each a silica nanoparticle where Z^{min} (nm) represents the distance between two centers of the liposomes at the equilibrium position

b_3	ϵ_r=1			ϵ_r=42.5			ϵ_r=80		
	E_3^{min}	Z^{min}	ξ_3	E_3^{min}	Z^{min}	ξ_3	E_3^{min}	Z^{min}	ξ_3
24.75	−2611.21	58.56	0.39	−3294.67	58.56	0.39	−3296.65	58.58	0.41
28.28	−3213.79	65.64	0.41	−3829.17	65.65	0.42	−3830.08	65.64	0.41
31.82	−3808.65	72.72	0.41	−4351.23	72.71	0.40	−4358.97	72.71	0.40
35.36	−4395.02	79.78	0.39	−4888.32	79.78	0.39	−4891.53	79.79	0.40

this, the electrostatic and the van der Waals energies were evaluated using the Coulombic and the Lennard-Jones functions, respectively. To allow a mathematical treatment, the continuum approach assumes that atoms in a molecule are uniformly distributed over a surface or throughout the volume of the molecule, and then an integration approach was applied to evaluate the total energy of the system. We assumed that silica nanoparticles can be modeled as perfect spheres consisting of SiO_2 beads, and the liposome is composed of a dipalmitoylphosphatidylcholine (DPPC) lipid bilayer. For this we derived analytical expressions to describe how the various energies depend on the particle sizes and the distances between particles.

We considered two systems that are (i) one liposome containing two silica nanoparticles and (ii) two liposomes each encapsulating a silica nanoparticle. The total surface areas of the liposomes in the two systems were assumed to be equal where the silica radius is fixed to be 16 nm. The latter system has a lower energy level because the lipid shells fit more snugly around the nanoparticle. Therefore the encapsulation of single silica molecule entity in small liposomes may be found in experiments.

We found that the mutual compensation of the electrostatic dipoles on the lipid head groups and on the nanoparticle surface make the overall electrostatic contribution negligibly small. The balance of the van der Waals interactions does not consider the compensating interactions of solvent molecules. Hence, the touching configurations of nanoparticles with liposomes and among each other are preferred. Future work should aim at deriving a continuum model for the van der Waals interactions exerted by different types of solvent. It is well known that under physiological ion concentration of 100–150 mM, the ions and about four ordered water layers will form a counter-ion cloud that completely screens the membrane potential and even overcompensates the effect of the lipid charges [55]. Here, we neglected such atomistic effects. They could certainly be integrated in the continuum description used here by adjusting the attractive and the repulsive Lennard-Jones constants. However, we emphasize that this work considered particle dimensions at a much larger scale. It would be highly desirable if suitable experimental data become available on the binding constants of nanoparticles to biological membranes that could be used for calibrating the computational results presented here.

Our work thus could be viewed as a first step toward the study of transport behavior of nanoparticles through or inside cells where general analytic expressions for the total molecular energy of the system are obtained.

Acknowledgments This work was supported by a postdoctoral fellowship to DB by the Alexander von Humboldt Foundation. The authors thank Dr. Tihamér Geyer for many helpful discussions and Dr. Michael Hutter for helpful comments on the manuscript.

Appendix

The expressions of the interaction energy for both Coulombic and Lennard-Jones potentials are given in this appendix.

A: Electrostatic energy

The electrostatic energy between the inner and the outer head groups and the nanoparticle, utilizing double surface integrals for concentric spheres or for offset of concentric spheres, is given by

$$\begin{aligned} Q_1(a,b) \quad &= \tfrac{D\eta_{sh}(b)e^2}{4\pi}\left[\tfrac{1}{\epsilon_0\epsilon_r}-\tfrac{1}{2}\left(1-\tfrac{1}{\epsilon_r}\right)\right]\left[\tfrac{1}{2}(0.3)(1)L^{Q}_{1/2}(a,b)\right. \\ &+\tfrac{1}{2}(-0.3)(1)L^{Q}_{1/2}(a+0.161,b)+\tfrac{1}{2}(0.3)(-1)L^{Q}_{1/2}(a,b+0.05) \\ &+\tfrac{1}{2}(-0.3)(-1)L^{Q}_{1/2}(a+0.161,b+0.05)+\tfrac{1}{2}(0.3)(1)L^{Q}_{1/2}(a,b+4.336) \\ &+\tfrac{1}{2}(-0.3)(1)L^{Q}_{1/2}(a+0.161,b+4.336)+\tfrac{1}{2}(0.3)(-1)L^{Q}_{1/2}(a,b+4.286) \\ &\left.+\tfrac{1}{2}(-0.3)(-1)L^{Q}_{1/2}(a+0.161,b+42.86)\right], \end{aligned} \tag{A1}$$

where e denotes an elementary charge, D represents a dangling atom density of 1 nm^{-2} for both silicon and oxygen and $L^{Q}_{1/2}(a,b)$ is given by (4). The rational coefficients come from the proportional content of 1/2 choline and 1/2 phosphate groups in the head group. The charge values are as given in Table 1.

The electrostatic energy between two offset spheres for the SiO_2 nanoparticles is given by

$$\begin{aligned} Q_2(a) \quad &= \tfrac{D^2e^2}{4\pi}\left[\tfrac{1}{\epsilon_0\epsilon_r}-\tfrac{1}{2}\left(1-\tfrac{1}{\epsilon_r}\right)\right]\left[(0.3)(0.3)K^{Q}_{1/2}(a,a)\right. \\ &+(-0.3)(-0.3)K^{Q}_{1/2}(a+0.161,a+0.161) \\ &\left.+2(0.3)(-0.3)K^{Q}_{1/2}(a,a+0.161)\right], \end{aligned} \tag{A2}$$

where $K^{Q}_{1/2}(a,b)$ is given by (3), and a and a+0.161 denote the radii of the probability distribution of silicon and oxygen atoms, respectively.

The electrostatic energy between two offset spherical liposomes is given by

$$\begin{aligned} Q_3(a,b) &= Q_3^*(b, b+0.05) + Q_3^*(b+4.286, b+4.336) \\ &\quad +2Q_3^{**}(b, b+0.05, b+4.286, b+4.336), \end{aligned} \tag{A3}$$

where

$$\begin{aligned} Q_3^*(a,b) &= \tfrac{\eta_{sh}(a)\eta_{sh}(b)e^2}{4\pi}\left[\tfrac{1}{\epsilon_0\epsilon_r} - \tfrac{1}{2}\left(1-\tfrac{1}{\epsilon_r}\right)\right]\left[\tfrac{1}{4}(1)(1)K_{1/2}^{Q}(a,a)\right. \\ &\quad \left.+\tfrac{1}{4}(-1)(-1)K_{1/2}^{Q}(b,b) + 2\left(\tfrac{1}{4}\right)(1)(-1)K_{1/2}^{Q}(a,b)\right], \end{aligned}$$

and

$$\begin{aligned} Q_3^{**}(a,b) &= \tfrac{\eta_{sh}(a)\eta_{sh}(d)e^2}{4\pi}\left[\tfrac{1}{\epsilon_0\epsilon_r} - \tfrac{1}{2}\left(1-\tfrac{1}{\epsilon_r}\right)\right]\left[\tfrac{1}{4}(1)(1)K_{1/2}^{Q}(a,d)\right. \\ &\quad +\tfrac{1}{4}(-1)(-1)K_{1/2}^{Q}(b,c) + \tfrac{1}{4}(1)(-1)K_{1/2}^{Q}(a,c) \\ &\quad \left.+\tfrac{1}{4}(-1)(1)K_{1/2}^{Q}(b,d)\right], \end{aligned}$$

and $K_{1/2}^{Q}(a,b)$ is defined by (3).

B: van der Waals energy

The van der Waals energy between a head group and the nanoparticle utilizing a surface integral for SiO_2 of radius a and a volume integral for the head group of the inner radius b and of the thickness 0.4 nm is given by

$$\begin{aligned} P_1(a,b) &= \eta_{silica}\eta_{vh}(b)\left[\tfrac{1}{6}\left(-A_{Si-Q_a}I_3\left[N_n^{LJ}(a,b,0.4)\right] + B_{Si-Q_a}I_6\left[N_n^{LJ}(a,b,0.4)\right]\right)\right. \\ &\quad +\tfrac{1}{6}\left(-A_{Si-Q_o}I_3\left[N_n^{LJ}(a,b,0.4)\right] + B_{Si-Q_o}I_6\left[N_n^{LJ}(a,b,0.4)\right]\right) \\ &\quad +\tfrac{2}{6}\left(-A_{O-Q_a}I_3\left[N_n^{LJ}(a,b,0.4)\right] + B_{O-Q_a}I_6\left[N_n^{LJ}(a,b,0.4)\right]\right) \\ &\quad \left.+\tfrac{2}{6}\left(-A_{O-Q_o}I_3\left[N_n^{LJ}(a,b,0.4)\right] + B_{O-Q_o}I_6\left[N_n^{LJ}(a,b,0.4)\right]\right)\right], \end{aligned} \tag{B1}$$

where A_{1-2} and B_{1-2} are the Lennard-Jones attractive and repulsive constants, respectively, obtained by the mixing rule. The function $N_n^{LJ}(a,b,0.4)$ is defined by (11) where n is a positive integer corresponding to the power of the polynomials appearing in integrals I_3 and I_6 defined by (6) and (7). Again, the rational coefficients come from the proportional content of 1/2 choline and 1/2 phosphate groups in the head group, and of 1/3 silicon and 2/3 oxygen atoms in the silica nanoparticle.

The van der Waals energy between the intermediate layer and the nanoparticle utilizing double surface integrals for concentric spheres where the radius of SiO_2 (intermediate layer) is assumed to be *a (b)* is given by

$$\begin{aligned} P_2(a,b) &= \eta_{silica}\eta_{si}(b)\left[\tfrac{1}{3}\left(-A_{Si-N_a}I_3\left[L_n^{LJ}(a,b)\right] + B_{Si-N_a}I_6\left[L_n^{LJ}(a,b)\right]\right)\right. \\ &\quad \left.+\tfrac{2}{3}\left(-A_{O-N_a}I_3\left[L_n^{LJ}(a,b)\right] + B_{O-N_a}I_6\left[L_n^{LJ}(a,b)\right]\right)\right], \end{aligned} \tag{B2}$$

where $L_n^{LJ}(a,b)$ is given by (9) and n is a positive integer corresponding to the power of I_3 and I_6 defined by (6) and (7).

The van der Waals energy between the tail group and the nanoparticle utilizing a surface integral for SiO_2 of radius a and a volume integral for the tail group of the inner radius b and of the thickness 1.6 nm is given by

$$\begin{aligned} P_3(a,b) &= \eta_{silica}\eta_{vt}(b)\left[\tfrac{1}{3}\left(-A_{Si-C_1}I_3\left[N_n^{LJ}(a,b,1.6)\right] + B_{Si-C_1}I_6\left[N_n^{LJ}(a,b,1.6)\right]\right)\right. \\ &\quad \left.+\tfrac{2}{3}\left(-A_{O-C_1}I_3\left[N_n^{LJ}(a,b,1.6)\right] + B_{O-C_1}I_6\left[N_n^{LJ}(a,b,1.6)\right]\right)\right], \end{aligned} \tag{B3}$$

where $N_n^{LJ}(a,b,1.6)$ is defined by (11) with corresponding values of n.

In the case when the inner sphere moves away from the origin to the distance x, the van der Waals energy between a head group and the inner nanoparticle utilizing a surface integral for SiO_2 of radius a and a volume integral for the head group of inner radius b and of thickness 0.4 nm is given by

$$\begin{aligned} P_4(a,b) &= \eta_{silica}\eta_{vh}(b)\left[\tfrac{1}{6}\left(-A_{Si-Q_a}I_3\left[O_n^{LJ}(a,b,0.4)\right] + B_{Si-Q_a}I_6\left[O_n^{LJ}(a,b,0.4)\right]\right)\right. \\ &\quad +\tfrac{1}{6}\left(-A_{Si-Q_o}I_3\left[O_n^{LJ}(a,b,0.4)\right] + B_{Si-Q_o}I_6\left[O_n^{LJ}(a,b,0.4)\right]\right) \\ &\quad +\tfrac{2}{6}\left(-A_{O-Q_a}I_3\left[O_n^{LJ}(a,b,0.4)\right] + B_{O-Q_a}I_6\left[O_n^{LJ}(a,b,0.4)\right]\right) \\ &\quad \left.+\tfrac{2}{6}\left(-A_{O-Q_o}I_3\left[O_n^{LJ}(a,b,0.4)\right] + B_{O-Q_o}I_6\left[O_n^{LJ}(a,b,0.4)\right]\right)\right], \end{aligned} \tag{B4}$$

where $O_n^{LJ}(a,b,0.4)$ is defined by (12) and n is a positive integer corresponding to the power of the polynomials appearing in integrals I_3 and I_6 defined by (6) and (7).

The van der Waals energy between the intermediate layer and the nanoparticle utilizing double surface integrals for an offset of concentric sphere shown in Fig. 1(d), with the radius of SiO_2 (intermediate layer) assumed to be *a (b)* is given by

$$P_5(a,b)= \eta_{silica}\eta_{si}(b)\left[\tfrac{1}{3}\left(-A_{Si-N_a}I_3\left[M_n^{LJ}(a,b)\right]+B_{Si-N_a}I_6\left[M_n^{LJ}(a,b)\right]\right)\right. \quad \left.+\tfrac{2}{3}\left(-A_{O-N_a}I_3\left[M_n^{LJ}(a,b)\right]+B_{O-N_a}I_6\left[M_n^{LJ}(a,b)\right]\right)\right], \quad \text{(B5)}$$

where $M_n^{LJ}(a,b)$ is given by (10) and n is a positive integer corresponding to the power of I_3 and I_6 defined by (6) and (7).

Once the silica nanoparticle moves away from the origin by distance x, the van der Waals energy between the tail group and the nanoparticle utilizing a surface integral for SiO_2 of radius a and a volume integral for the tail group of the inner radius b and of the thickness 1.6 nm is given by

$$\begin{aligned} P_6(a,b) \quad &= \eta_{silica}\eta_{vt}(b)\left[\tfrac{1}{3}\left(-A_{Si-C_1}I_3\left[O_n^{LJ}(a,b,1.6)\right]+B_{Si-C_1}I_6\left[O_n^{LJ}(a,b,1.6)\right]\right)\right. \\ &\quad \left.+\tfrac{2}{3}\left(-A_{O-C_1}I_3\left[O_n^{LJ}(a,b,1.6)\right]+B_{O-C_1}I_6\left[O_n^{LJ}(a,b,1.6)\right]\right)\right], \end{aligned} \quad \text{(B6)}$$

where $O_n^{LJ}(a,b,1.6)$ is defined by (12) with corresponding values of n.

The van der Waals energy between two offset spheres for the SiO_2 nanoparticles is given by

$$\begin{aligned} P_7(a,b) \quad &= \eta_{silica}^2\left[\tfrac{1}{9}\left(-A_{Si-Si}I_3\left[K_n^{LJ}(a,a)\right]+B_{Si-Si}I_6\left[K_n^{LJ}(a,a)\right]\right)\right. \\ &\quad +\tfrac{4}{9}\left(-A_{O-O}I_3\left[K_n^{LJ}(b,b)\right]+B_{O-O}I_6\left[K_n^{LJ}(b,b)\right]\right) \\ &\quad \left.+2\left(\tfrac{2}{9}\right)\left(-A_{Si-O}I_3\left[K_n^{LJ}(a,b)\right]+B_{Si-O}I_6\left[K_n^{LJ}(a,b)\right]\right)\right], \end{aligned} \quad \text{(B7)}$$

where $K_n^{LJ}(a,b)$ is defined by (8) with corresponding values of n appearing in (6) and (7), and a and b represent the radii of the probability distribution of silicon and oxygen atoms, respectively, in silica nanoparticle.

The van der Waals energy between two offset spheres of liposomes encapsulating silica nanoparticles is given by

$$\begin{aligned} P_8(a,b) \quad &= \eta_{sh}(a)\eta_{sh}(b)\left[\tfrac{1}{4}\left(-A_{Q_a-Q_a}I_3\left[K_n^{LJ}(a,a)\right]+B_{Q_a-Q_a}I_6\left[K_n^{LJ}(a,a)\right]\right)\right. \\ &\quad +\tfrac{1}{4}\left(-A_{Q_o-Q_o}I_3\left[K_n^{LJ}(b,b)\right]+B_{Q_o-Q_o}I_6\left[K_n^{LJ}(b,b)\right]\right) \\ &\quad \left.+2\left(\tfrac{1}{4}\right)\left(-A_{Q_a-Q_o}I_3\left[K_n^{LJ}(a,b)\right]+B_{Q_a-Q_o}I_6\left[K_n^{LJ}(a,b)\right]\right)\right], \end{aligned} \quad \text{(B8)}$$

where $K_n^{LJ}(a,b)$ is defined by (8) with corresponding values of n appearing in (6) and (7), and a and b denote the radii of choline and phosphate groups, respectively.

References

1. Chen M, von Mikecz A (2005) Exp Cell Res 305:51
2. Nel AE, Mädler L, Velegol D, Xia T, Hoek EMV, Somasundaran P, Klaessig F, Castranova V, Thompson M (2009) Nat Meter 8:543
3. Conner SD, Schmid SL (2003) Nature 422:37
4. Dohertyand GJ, McMahon HT (2009) Annu Rev Biochem 78:857
5. Zhao F, Zhang Y, Liu Y, Chang X, Chen C, Zhao Y (2011) Small 7:1322
6. Stayton I, Winiarz J, Shannon K, Ma Y (2009) Anal Bioanal Chem 394:1595
7. Xing X, He X, Peng J (2005) J Nanosci Nanotechnol 5:1688
8. Cho EC, Xie J, Wurm PA, Xia Y (2009) Nano Lett 9:1080
9. Limbach LK, Li Y, Grass RN, Brunner TJ, Hintermann MA, Muller M, Gunther D, Stark WJ (2005) Environ Sci Technol 39:9370
10. Schübbe S, Cavelius C, Schumann C, Koch M, Kraegeloh A (2010) Adv Eng Mater 12:417
11. Schübbe S, Schumann C, Cavelius C, Koch M, Mueller T, Kraegeloh A (2012) Chem Mater 24:914
12. Heller MJ (2002) Annu Rev Biomed Eng 4:129
13. Slowing II, Vivero-Escoto JL, Wu CW, Lin VSY (2008) Adv Drug Deliv Rev 60:1278
14. Kneuer C, Sameti M, Bakowsky U, Schiestel T, Schirra H, Schmidt H, Lehr CM (2000) Bioconjugate Chem 11:926
15. Luo D, Han E, Belcheva N, Saltzman WM (2004) J Contr Release 95:333
16. Radu DR, Lai CY, Jeftinija K, Rowe EW, Jeftinija S, Lin VSY (2004) J Am Chem Soc 126:1321
17. Roy I, Ohulchanskyy TY, Bharali DJ, Pudavar HE, Mistretta RA, Kaur N, Prasad P (2005) Proc Natl Acad Sci USA 102:279
18. Bharali DJ, Klejbor I, Stachowiak EK, Dutta P, Roy I, Kaur N, Bergey EJ, Prasad PN, Stachowiak MK (2005) Proc Natl Acad Sci USA 102:11539
19. Xia T, Kovochich M, Liong M, Meng H, Kabehie S, George S, Zink JI, Nel AE (2009) ACS Nano 3:3273
20. Slowing II, Trewyn BG, Giri S, Lin VSY (2007) Adv Funct Mater 17:1225
21. Chen JF, Ding HM, Wang JX, Shao L (2004) Biomaterials 25:723
22. Vivero-Escoto JL, Slowing II, Trewyn BG, Lin VSY (2010) Small 6:1952
23. Schumann C, Schübbe S, Cavelius C, Kraegeloh A (2012) J Biophotonics 5:117
24. Lieber M, Todaro G, Smith B, Szakal A, Nelson-Rees W (1976) Int J Cancer 17:62
25. Peckys D, de Jonge N (2011) Nano Lett 11:1733
26. Malvindi MA, Brunetti V, Vecchio G, Galeone A, Cingolanib R, Pompa PP (2012) Nanoscale 4:486
27. Sackmann E (1994) FEBS Lett 346:3
28. Foldvari M, Gesztes A, Mezei M (1990) J Microencapsul 7:479
29. Puyal C, Milhaud P, Bienvenüe A, Philippot JR (1995) Eur J Biochem 228:697
30. Mohanraj VJ, Barnes TJ, Prestidge CA (2010) Int J Pharmaceut 392:285
31. Ash WL, Zlomislic MR, Oloo EO, Tieleman DP (2004) Biochim Biophys Acta 1666:158

32. Berkowitz ML, Bostick DL, Pandit S (2006) Chem Rev 106:1527
33. Siu SWI, Vácha R, Jungwirth P, Böckmann RA (2008) J Chem Phys 128:125103
34. Wong-Ekkabut J, Baoukina S, Triampo W, Tang IM, Tieleman DP, Monticelli L (2008) Nat Nanotechnol 3:363
35. Marrink SJ, Risselada HJ, Yefimov S, Tieleman DP, de Vries AH (2007) J Phys Chem B 111:7812
36. Shelley JC, Shelley MY, Reeder RC, Bandyopadhyay S, Moore PB, Klein ML (2001) J Phys Chem B 105:9785
37. Wallace EJ, Sansom MSP (2007) Nano Lett 7:1923
38. Shinoda W, DeVane R, Klein ML (2010) J Phys Chem B 114:6836
39. Girifalco LA, Hodak M, Lee RS (2000) Phys Rev B 62:13104
40. Hodak M, Girifalco LA (2001) Chem Phys Lett 350:405
41. Cox BJ, Thamwattana N, Hill JM (2007) Proc Roy Soc A 463:461
42. Cox BJ, Thamwattana N, Hill JM (2007) Proc Roy Soc A 463:477
43. Baowan D, Cox BJ, Hill JM (2012) J Mol Model 18:549
44. Qian D, Liu WK, Ruoff RS (2001) J Phys Chem B 105:10753
45. Liu P, Zhang YW, Lu C (2005) J Appl Phys 97:094313
46. Patwardhan SV, Patwardhan G, Perry CC (2007) J Mater Chem 17:2875
47. Still WC, Tempczyk A, Hawley RC, Hendrickson T (1990) J Am Chem Soc 112:6127
48. Hirschfelder JO, Curtiss CF, Bird RB (1954) Molecular theory of gases and liquids. Wiley, New York
49. Cruz-Chu ER, Aksimentiev A, Schulten K (2006) J Phys Chem B 110:21497
50. Dorota N, Leen T, Dominique L, Johan M, Peter H (2010) Part Fibre Toxicol 7:39
51. Zhuravlev LT (2000) Colloid Surface Physicochem Eng Aspect 173:1
52. Makimura D, Metin C, Kabashima T, Matsuoka T, Nguyen QP, Miranda CR (2010) J Mater Sci 45:5084
53. Petrache HI, Feller SE, Nagle JF (1997) Biophys J 70:2237
54. Chu Z, Huang Y, Taob Q, Li Q (2011) Nanoscale 3:3291
55. Lin JH, Baker NA, McCammon JA (2002) Biophys J 83:1374